Noname manuscript No.
(will be inserted by the editor)

Two-qubit state recovery from amplitude damping based on weak measurement

Sajede Harraz · **Shuang Cong** · **Kezhi Li**

Received: date / Accepted: date

Abstract In this paper, we propose a feed-forward control approach to protect arbitrary two-qubit pure and mixed initial states using the weak measurement. A feed-forward operation and measurements are used before the noise channel, and afterwards a reversed operation and measurements are applied to recover the state back to its initial state. In the case of two-qubit pure states, we use the unraveling trick to describe the state of the system in each step of the control procedure. For two-qubit mixed states, a completely-positive trace-preserving (CPTP) map is implemented. Finally, the fidelity and success probability are used to evaluate the effect of protection. The complete recovery conditions for the measurement strengths are derived, under which we achieve the optimal fidelity and the success probability of recovering the initial pure and mixed states.

Keywords Quantum control · State protection · Amplitude damping · Quantum measurement

This work was supported by the National Natural Science Foundation of China under grant no. 61973290 and 61720106009.

S. Harraz
University of Science and Technology of China, Department of Automation, Hefei 230027, China
E-mail: sajede@ustc.edu.cn

S. Cong
University of Science and Technology of China, Department of Automation, Hefei 230027, China
E-mail: scong@ustc.edu.cn

K. Li
University College London, Institute of Health information, London, NW1 2DA, UK
E-mail: Ken.li@ucl.ac.uk

1 Introduction

The dynamic of open quantum systems becomes decoherent easily due to the inevitable interaction with the environment [1]. To suppress the effect of decoherence, various strategies have been studied, such as decoherence-free subspaces [2], quantum error correction [3–7], quantum feedback control (QFBC) [8–11] and quantum feed-forward control (QFFC) [12–14]. In both quantum feedback control and quantum feed-forward control, the measurement plays an important role. The measurement in quantum theory significantly differs from that in classical theory. In quantum measurement there is a trade-off between the information gain and the disturbance of the system caused by the measurement [15]. Hence, the quantum weak measurement technique is promising, since it has little effect on the dynamic of the quantum system. Weak measurements generalize ordinary quantum measurements, and they reveal some information about the quantum state. This process is achieved by leveraging a weak coupling between the measurement device and the system.

Amplitude damping is a major decoherence that occurs in many quantum systems [16], such as a photon qubit in a leaky cavity, an atomic qubit subjected to spontaneous decay, or a super-conduction qubit with zero-temperature energy relaxation. The specific control problem we are interested in here is the stabilisation against amplitude damping for two-qubit pure and mixed states. Similar problems have been considered for one qubit quantum state recovery based on the QFBC and QFFC. A quantum feedback control scheme was proposed in [16], which included quantum weak measurement and correction rotation based on the result of the measurements after the noise channel; and it was experimentally implemented [17]. This scheme was studied for different initial states, measurements and feedback control bases [18–20]. Furthermore, it has been illustrated that one-qubit state affected by amplitude damping can be completely recovered through applying feed-forward control [12]. Feed-forward control has been applied to make the state of the system immune to the effect of an amplitude damping channel. A feed-forward control (FFC) technique was used to realize a better impact of the discrimination of two nonorthogonal states after passing an amplitude damping channel [21]. Also, a quantum composite control scheme was proposed [22], where quantum feedback control and quantum feed-forward control were combined for protecting two nonorthogonal states of a two-level quantum system against the amplitude damping noise. Most of the previous works on quantum state protection using quantum feed-forward control focused on protocols for pure states [21,22], and none has addressed the issue of protecting arbitrary mixed states. The QFFC scheme is a probabilistic scheme which includes the success probability in addition to the fidelity to evaluate the performance of the control scheme. The QFBC and QFFC were mathematically studied to solve the problem of protecting the completely unknown states against given noise [13, 14]. In fact, one essentially cannot suppress any given noise by using only QFBC. In other words, if the initial state is unknown, only the unitary rotational part of noise can be eliminated. In the QFFC control scheme, it was shown that if the noise is weak, the best control scheme is to leave the state of the system unchanged; In case of intense noise, one needs to measure the system before noise and after the noise, based on the result of the measurement, reconstruct the state. Similar problems were

considered for two-qubit quantum state recovery based on quantum gates [23]. An arbitrary two-qubit pure state under amplitude damping in a weak measurement was probabilistically recovered using Hadamard and CNOT gates. However, their scheme cannot recover some states, in which they solved it by adding a step before the noise to prepare the system in a more robust state. Later, the authors used the same method to protect an arbitrary two-qubit mixed state [24]. In the case of protecting two-qubit system, a feedback control to control entanglement in open quantum system by using a feedback action which relies on local operations and classical communication was proposed [8]. However, this method is not optimal. Later an optimal feedback control was found [9] by first gaining insights from the subsystem purity and then by numerical analysis of the concurrence. This method is dependent on the initial state. Furthermore, the universal optimal Markovian feedback control was considered to control the entanglement of two-qubit [10], which is optimal and independent of the initial state. In 2017, we studied the optimal control of quantum state transfer in a two-dimensional quantum system by a sequence of non-selective projection measurements. In that work we indicated that for a given initial state, one can always find the corresponding projection operator that can effectively drive the given initial state to any pure state. An external control field was proposed to compensate the effect of the free evolution of system [15]. In 2018, we studied the possibility of protecting the mixed state of a quantum system that went through noise by weak measurements and control operations [20]. In 2019, we studied the suppression of phase damping in two cases: there is and isn't the y component in initial state and deduced the optimal parameters and performances of the control schemes for the various initial state situations [25].

In this paper, we consider the feed-forward control scheme for recovering arbitrary pure and mixed initial two-qubit states. We use the pre-weak measurement to gain information about the initial state. Then to make the states almost immune to the amplitude damping channel, we apply feed-forward operation based on the result of measurements. After the noise channel, we restore the initial state; hence, a reversed unitary operation and a post-weak measurement are applied. For mixed initial states, we propose a completely-positive trace-preserving (CPTP) map to describe the recovery control and final state of the system. We use the Monte-Carlo method over a large ensemble of initial states in experimental simulations to prove the effectiveness of feed-forward control for any arbitrary two-qubit initial state. Furthermore, we compare the feed-forward control for two-qubit with the method in [23], and prove that feed-forward control proposed in this paper has much better performance.

The paper's structure is arranged as follows. In Sect. 2 the feed-forward recovery control for pure and mixed initial states based on weak measurement is studied. Moreover, the complete recovery condition under which one can completely recover the state of the system is given. In Sect. 3 the numerical experiments for general recovery and complete recovery control and their comparisons are given. Finally, the conclusion is drawn in Sect. 4.

2 Weak measurement based Feed-forward recovery control

The control task in this paper is to bring the state of the system after passing through the noise channel back to its initial state as close as possible before being affected by noise. To achieve this, the feed-forward control procedure consists of two parts: a) before and b) after the noise channel parts. Before the noise channel, the pre-weak measurement is applied to gain some information about the initial state. Then the feed-forward operations are used to change the state in a way to reduce the effects of the noise. Amplitude damping leaves the ground states unchanged and decays the excited states by its decaying rate. Hence, the feed-forward operations need to bring the states close to ground state of the noise channel. After the noise channel, the reversed operations are applied to retrieve the information of the initial state. The schematic diagram of the feed-forward recovery control is given in Fig. 1, which consists of five steps. In the following, we give and analyze the detail formulas in each steps for both pure and mixed initial states.

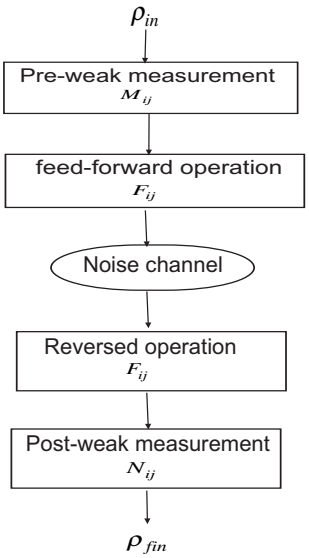

Fig. 1 Schematic diagram of the feed-forward recovery control scheme.

2.1 Two-qubit pure initial state

An arbitrary two-qubit pure initial state can be written as:

$$|\psi_{in}\rangle = \alpha|00\rangle + \beta|01\rangle + \gamma|10\rangle + \delta|11\rangle \tag{1}$$

where $|0\rangle = \begin{pmatrix} 1 \\ 0 \end{pmatrix}$ and $|1\rangle = \begin{pmatrix} 0 \\ 1 \end{pmatrix}$.

We intend to protect this state from the noise by means of the feed-forward recovery control according to five steps described in Fig. 1.

Table 1 Measurement operators and control operations used in two-qubit feed-forward recovery control.

Pre-weak measurement	Unitary operation	Post-weak measurement
$M_{00}=\begin{pmatrix} p & 0 & 0 & 0 \\ 0 & \sqrt{p}\sqrt{1-p} & 0 & 0 \\ 0 & 0 & \sqrt{p}\sqrt{1-p} & 0 \\ 0 & 0 & 0 & 1-p \end{pmatrix}$	$F_{00}=\begin{pmatrix} 1&0&0&0 \\ 0&1&0&0 \\ 0&0&1&0 \\ 0&0&0&1 \end{pmatrix}$	$N_{00}=\begin{pmatrix} 1-q & 0 & 0 & 0 \\ 0 & \sqrt{1-q} & 0 & 0 \\ 0 & 0 & \sqrt{1-q} & 0 \\ 0 & 0 & 0 & 1 \end{pmatrix}$
$M_{01}=\begin{pmatrix} \sqrt{p}\sqrt{1-p} & 0 & 0 & 0 \\ 0 & p & 0 & 0 \\ 0 & 0 & 1-p & 0 \\ 0 & 0 & 0 & \sqrt{p}\sqrt{1-p} \end{pmatrix}$	$F_{01}=\begin{pmatrix} 0&1&0&0 \\ 1&0&0&0 \\ 0&0&0&1 \\ 0&0&1&0 \end{pmatrix}$	$N_{01}=\begin{pmatrix} \sqrt{1-q} & 0 & 0 & 0 \\ 0 & 1-q & 0 & 0 \\ 0 & 0 & 1 & 0 \\ 0 & 0 & 0 & \sqrt{1-q} \end{pmatrix}$
$M_{10}=\begin{pmatrix} \sqrt{p}\sqrt{1-p} & 0 & 0 & 0 \\ 0 & 1-p & 0 & 0 \\ 0 & 0 & p & 0 \\ 0 & 0 & 0 & \sqrt{p}\sqrt{1-p} \end{pmatrix}$	$F_{10}=\begin{pmatrix} 0&0&1&0 \\ 0&0&0&1 \\ 1&0&0&0 \\ 0&1&0&0 \end{pmatrix}$	$N_{10}=\begin{pmatrix} \sqrt{1-q} & 0 & 0 & 0 \\ 0 & 1 & 0 & 0 \\ 0 & 0 & 1-q & 0 \\ 0 & 0 & 0 & \sqrt{1-q} \end{pmatrix}$
$M_{11}=\begin{pmatrix} 1-p & 0 & 0 & 0 \\ 0 & \sqrt{p}\sqrt{1-p} & 0 & 0 \\ 0 & 0 & \sqrt{p}\sqrt{1-p} & 0 \\ 0 & 0 & 0 & p \end{pmatrix}$	$F_{11}=\begin{pmatrix} 0&0&0&1 \\ 0&0&1&0 \\ 0&1&0&0 \\ 1&0&0&0 \end{pmatrix}$	$N_{11}=\begin{pmatrix} 1 & 0 & 0 & 0 \\ 0 & \sqrt{1-q} & 0 & 0 \\ 0 & 0 & \sqrt{1-q} & 0 \\ 0 & 0 & 0 & 1-q \end{pmatrix}$

Step 1: In the first step we need to obtain some information about the initial state by performing pre-weak measurement as: $\Pi_{00}=M_{00}^{\dagger}M_{00}$, $\Pi_{01}=M_{01}^{\dagger}M_{01}$, $\Pi_{10}=M_{10}^{\dagger}M_{10}$ and $\Pi_{11}=M_{11}^{\dagger}M_{11}$ where the measurement operators $M_{ij}(i,j=0,1)$ are given in Table 1, and $p\in[0,1]$ is the pre-weak measurement strength. The state of the system $|\psi_{in}\rangle$ after being measured by the pre-weak measurements M_{ij} becomes $\left|\psi_{M_{ij}}\right\rangle$ as:

$$\left|\psi_{M_{ij}}\right\rangle=\frac{M_{ij}|\psi_{in}\rangle}{\sqrt{\langle\psi_{in}|\,M_{ij}^{\dagger}M_{ij}\Big|\,\psi_{in}\rangle}} \tag{2}$$

with probability $g_{M_{ij}}=\langle\psi_{in}|\,M_{ij}^{\dagger}M_{ij}\Big|\,\psi_{in}\rangle$.

Step 2: The feed-forward operation is applied based on the result of the pre-weak measurement. The feed-forward operation brings the qubit closer to the ground state and makes them less vulnerable to the amplitude damping. The feed-forward operators are given in Table. 1. When the result according to M_{00} is acquired, the system is in the ground state and it is immune to the amplitude damping. We apply the identity operator as F_{00} to keep the state unchanged. As the result according to M_{ij} is acquired, the corresponding F_{ij} is chosen as the feed-forward operation. The state of the system $\left|\psi_{M_{ij}}\right\rangle$ after the feed-forward operation is given by $\left|\psi_{F_{ij}}\right\rangle$:

$$\left|\psi_{F_{ij}}\right\rangle=F_{ij}\left|\psi_{M_{ij}}\right\rangle \tag{3}$$

Step 3: The Two-qubit goes through the amplitude damping noise channel. The amplitude damping of a single qubit can be represented by Kraus operators as $e_0=\begin{pmatrix}1&0\\0&\sqrt{1-r}\end{pmatrix}$, $e_1=\begin{pmatrix}0&\sqrt{r}\\0&0\end{pmatrix}$, where $r\in[0,1]$ is the possibility of decaying of the

excited state [26]. For a two-qubit we assume that amplitude damping occurs for both qubits locally and independently but with the same decaying rate $r = r_1 = r_2$. Therefore the amplitude-damping process for the whole two-qubit system can be described by four Kraus operators $(e_{mn},\ m,n = 0,1)$ as:

$$\begin{aligned}
e_{00} = e_0 \otimes e_0 &= \begin{pmatrix} 1 & 0 & 0 & 0 \\ 0 & \sqrt{1-r} & 0 & 0 \\ 0 & 0 & \sqrt{1-r} & 0 \\ 0 & 0 & 0 & 1-r \end{pmatrix} \\
e_{01} = e_0 \otimes e_1 &= \begin{pmatrix} 0 & \sqrt{r} & 0 & 0 \\ 0 & 0 & 0 & 0 \\ 0 & 0 & 0 & \sqrt{r}\sqrt{1-r} \\ 0 & 0 & 0 & 0 \end{pmatrix} \\
e_{10} = e_1 \otimes e_0 &= \begin{pmatrix} 0 & 0 & \sqrt{r} & 0 \\ 0 & 0 & 0 & \sqrt{r}\sqrt{1-r} \\ 0 & 0 & 0 & 0 \\ 0 & 0 & 0 & 0 \end{pmatrix} \\
e_{11} = e_1 \otimes e_1 &= \begin{pmatrix} 0 & 0 & 0 & r \\ 0 & 0 & 0 & 0 \\ 0 & 0 & 0 & 0 \\ 0 & 0 & 0 & 0 \end{pmatrix}
\end{aligned} \tag{4}$$

The state of the system $\left|\psi_{F_{ij}}\right\rangle$ in Eq. (3) after passing through the noise channel is not pure anymore. But to make the calculation more manageable, we use a mathematical technique called unraveling. So the qubit trajectories can be divided into two parts, 'jump' and 'no jump' trajectories, and each qubit can jump to state $|0\rangle$, or 'no jump' happens. If both qubits jump, the system state becomes $|\psi^{e_{11}}\rangle = |00\rangle$ with probability $g_{e_{11}} = \left\langle \psi_{F_{ij}} \right| e_{11}^{\dagger} e_{11} \left| \psi_{F_{ij}} \right\rangle$, which is non-invertible. If 'no jump' scenario happens for at least one of the qubits, the state of the system transforms to $|\psi^{e_{mn}}\rangle = \frac{e_{mn}\left|\psi_{F_{ij}}\right\rangle}{\sqrt{\left\langle \psi_{F_{ij}} \right| e_{mn}^{\dagger} e_{mn} \left| \psi_{F_{ij}} \right\rangle}}$ with probability $g_{e_{mn}} = \left\langle \psi_{F_{ij}} \right| e_{mn}^{\dagger} e_{mn} \left| \psi_{F_{ij}} \right\rangle$ and we can recover the state of the system.

Step 4: After the noise channel, the reversed operations F_{ij}, which are the same as the ones in step 2, are applied based on the feed-forward operations. The state of the system after using the reversed operation becomes

$$\left|\psi_{F_{ij}}^{e_{mn}}\right\rangle = F_{ij}|\psi^{e_{mn}}\rangle \tag{5}$$

Step 5: We retrieve the information of the initial state by means of post-weak measurement in a way that $M_{ij}N_{ij}$ is almost proportionate to I. The post-weak measurement operators N_0 and N_1 are from the complete measurement sets $\left\{N_0, \overline{N_0}\right\}$ and $\left\{N_1, \overline{N_1}\right\}$, respectively, as:

$$\begin{aligned}
N_0 &= \begin{pmatrix} \sqrt{1-q_0} & 0 \\ 0 & 1 \end{pmatrix}, \overline{N}_0 = \begin{pmatrix} \sqrt{q_0} & 0 \\ 0 & 0 \end{pmatrix} \\
N_1 &= \begin{pmatrix} 1 & 0 \\ 0 & \sqrt{1-q_1} \end{pmatrix}, \overline{N}_1 = \begin{pmatrix} 0 & 0 \\ 0 & \sqrt{q_1} \end{pmatrix}
\end{aligned} \tag{6}$$

where $N_0^\dagger N_0 + \overline{N}_0^\dagger \overline{N}_0 = I$ and $N_1^\dagger N_1 + \overline{N}_1^\dagger \overline{N}_1 = I$.

In our recovery control we just preserves the result of N_i, discard the result of $\overline{N}_i$ and normalize the final state at the end of recovery control process. The post-weak measurement operators for two-qubit with $q_0 = q_1 = q$ are given in Table. 1, where $q \in [0,1]$ is the post-weak measurement strength.

The state of the system after being measured by the post-weak measurement is presented as:

$$\left|\psi_{N_{ij}}^{e_{mn}}\right\rangle = \frac{N_{ij}\left|\psi_{F_{ij}}^{e_{mn}}\right\rangle}{\sqrt{\left\langle\psi_{F_{ij}}^{e_{mn}}\right| N_{ij}^\dagger N_{ij}\left|\psi_{F_{ij}}^{e_{mn}}\right\rangle}} \tag{7}$$

with probability $g_{N_{ij}}^{e_{mn}} = \left\langle\psi_{F_{ij}}^{e_{mn}}\right| N_{ij}^\dagger N_{ij}\left|\psi_{F_{ij}}^{e_{mn}}\right\rangle$.

Since we consider the damped state in two scenarios: 'jump' and 'no jump', the final state of the system corresponding to M_{ij} is given by:

$$\rho_{M_{ij}}^{fin} = \sum_{m,n=0}^{1} \frac{g_{N_{ij}}^{e_{mn}}\left|\psi_{N_{ij}}^{e_{mn}}\right\rangle\left\langle\psi_{N_{ij}}^{e_{mn}}\right|}{\sqrt{g_{N_{ij}}^{e_{mns}}}} \tag{8}$$

The success (selection) probability $g_{M_{ij}}^{fin}$ for each weak measurement operator is:

$$g_{M_{ij}}^{fin} = \sum_{m,n=0}^{1} g_{N_{ij}}^{e_{mn}} \tag{9}$$

The total success (selection) probability g_{total} after the whole process of recovery control for all weak measurement operators is:

$$g_{total} = g_{M_{00}}^{fin} + g_{M_{01}}^{fin} + g_{M_{10}}^{fin} + g_{M_{11}}^{fin} \tag{10}$$

We derive the total success probability as a function of pre-weak measurement strength p, post-weak measurement strength q and damping probability r as

$$g_{total}(p,q,r) = (pq + qr - pqr - 1)^2 \tag{11}$$

According to Eq. (11), the total success probability is not a function of initial state. In other words, initial state elements do not have any effects on the amount of total success probability.

The fidelity between the initial state $|\psi_{in}\rangle$ and the final state $\rho_{M_{ij}}^{fin}$ that corresponds to each weak measurement operator is: $Fid_{M_{ij}} = \langle\psi_{in}|\,\rho_{M_{ij}}^{fin}\left|\,\psi_{in}\right\rangle$. The total fidelity Fid_{total} for all weak measurement operators is calculated by the fidelity $Fid_{M_{ij}}$ as:

$$Fid_{total} = \frac{g_{M_{00}}^{fin} Fid_{M_{00}} + g_{M_{01}}^{fin} Fid_{M_{01}} + g_{M_{10}}^{fin} Fid_{M_{10}} + g_{M_{11}}^{fin} Fid_{M_{11}}}{g_{M_{00}}^{fin} + g_{M_{01}}^{fin} + g_{M_{10}}^{fin} + g_{M_{11}}^{fin}} \tag{12}$$

The final expression for total fidelity is too long, so the behavior of the fidelity is explained by numerical simulations in sec.III.

To better understand the control process, here we present an analytic expression only for measurement operator M_{00}. All the states corresponding to all measurement operators can be analytically obtained, although for brevity we do not bring them in this paper.

In the first step, we apply a pre-weak measurement defined by M_{ij}. Let us consider the result corresponding to M_{00} is acquired. The state of the system $|\psi_{in}\rangle$ in Eq. (1) after being measured by M_{00} becomes:

$$\begin{aligned}\left|\psi_{M_{00}}\right\rangle = M_{00}|\psi_{in}\rangle = \frac{1}{\sqrt{g_{M_{00}}}}\big(&\alpha p|00\rangle + \beta\sqrt{p}\sqrt{1-p}|01\rangle \\ &+ \gamma\sqrt{p}\sqrt{1-p}|10\rangle + \delta\sqrt{1-p}|11\rangle\big)\end{aligned} \tag{13}$$

where $g_{M_{00}} = \alpha^2 p^2 + \beta^2 p(1-p) + \gamma^2 p(1-p) + \delta^2 (p-1)^2$ is the probability of achieving the result according to measurement operator M_{00}.

Since the result corresponding to M_{00} happens, before noise we choose the feed-forward operation F_{00}, and leave the state unchanged. $\left|\psi_{F_{00}}\right\rangle$ is the state of the system after applying the feed-forward operation:

$$\left|\psi_{F_{00}}\right\rangle = F_{00}\left|\psi_{M_{00}}\right\rangle = \left|\psi_{M_{00}}\right\rangle \tag{14}$$

Now the two-qubit enters the noise channel. As we explained before, the state of the system 'jumps' into $|00\rangle$ state or 'no jump' happens. The 'jump' scenario for both qubits happens with probability $g_{e_{11}} = \left\langle\psi_{F_{ij}}\right| e_{11}^{\dagger} e_{11} \left|\psi_{F_{ij}}\right\rangle = |\delta|^2 r^2 (p-1)^2$, and the state of the system becomes $|\psi^{e_{11}}\rangle = |00\rangle$. Also, 'no jump' scenario for both qubits transfers the state into $|\psi^{e_{00}}\rangle$ as:

$$\begin{aligned}\left|\psi_{M_{01}}^{e_{00}}\right\rangle = \frac{1}{\sqrt{g_{e_{00}}}}\big(&\alpha p|00\rangle \\ &+ \beta\sqrt{p}\sqrt{1-p}\sqrt{1-r}|01\rangle \\ &+ \gamma\sqrt{p}\sqrt{1-p}\sqrt{1-r}|10\rangle \\ &+ \delta(1-p)(1-r)|11\rangle\big)\end{aligned} \tag{15}$$

where $g_{e_{00}} = |\alpha|^2 p^2 + (|\beta|^2 + |\gamma|^2)(p(1-p)(1-r)) + |\delta|^2 (1-p)^2 (1-r)^2$ is the probability of no jumping of both qubits after the noise channel. The state of the system in the case that just one of the qubits jumps is analyzed in appendix A. Here we calculate the states which both qubits jump or no jump. After the noise channel, we make the reversed operation F_{00}. Hence the state of the system from 'no jumping' trajectory becomes $\left|\psi_{F_{00}}^{e_{00}}\right\rangle = F_{00}|\psi^{e_{00}}\rangle = |\psi^{e_{00}}\rangle$, and the 'jump' trajectory becomes $\left|\psi_{F_{00}}^{e_{11}}\right\rangle = F_{00}|\psi^{e_{11}}\rangle = |00\rangle$.

At last the post-weak measurement is applied by using the measurement operator N_{00}. The state of the system from 'no jumping' scenario becomes:

$$\begin{aligned}\left|\psi_{N_{00}}^{e_{00}}\right\rangle = \frac{1}{\sqrt{g_{N_{00}}}}\big(&\alpha p\,(1-q)\,|00\rangle \\ &+\beta\sqrt{p}\sqrt{1-p}\sqrt{1-r}\sqrt{1-q}|01\rangle \\ &+\gamma\sqrt{p}\sqrt{1-p}\sqrt{1-r}\sqrt{1-q}|10\rangle \\ &+\delta(1-p)(1-r)|11\rangle\big)\end{aligned} \tag{16}$$

with probability $g_{N_{00}}^{e_{00}} = |\alpha|^2 p^2 (1-q)^2 + (|\beta|^2+|\gamma|^2)(p(1-p)(1-r)(1-q)) + |\delta|^2 (1-p)^2 (1-r)^2$.

The jumping state after post-weak measurement becomes $\left|\psi_{N_{00}}^{e_{11}}\right\rangle = |00\rangle$ with probability of $g_{N_{00}}^{e_{11}} = |\delta|^2 r^2 (1-p)^2 (1-q)^2$. The final state of the system corresponding to measurement operator M_{00} after passing through the whole control procedure is given by:

$$\begin{aligned}\rho_{M_{00}}^{fin} = &\frac{1}{g_{N_{00}}^{e_{00}} + g_{N_{00}}^{e_{01}} + g_{N_{00}}^{e_{10}} + g_{N_{00}}^{e_{11}}}\Big(g_{N_{00}}^{e_{00}}\left|\psi_{N_{00}}^{e_{00}}\right\rangle\left\langle\psi_{N_{00}}^{e_{00}}\right| \\ &+ g_{N_{00}}^{e_{01}}\left|\psi_{N_{00}}^{e_{01}}\right\rangle\left\langle\psi_{N_{00}}^{e_{01}}\right| + g_{N_{00}}^{e_{10}}\left|\psi_{N_{00}}^{e_{10}}\right\rangle\left\langle\psi_{N_{00}}^{e_{10}}\right| + g_{N_{00}}^{e_{11}}|00\rangle\langle 00|\Big)\end{aligned} \tag{17}$$

where $\left|\psi_{N_{00}}^{e_{01}}\right\rangle\left\langle\psi_{N_{00}}^{e_{01}}\right|$, $\left|\psi_{N_{00}}^{e_{10}}\right\rangle\left\langle\psi_{N_{00}}^{e_{10}}\right|$, $g_{N_{00}}^{e_{01}}$, and $g_{N_{00}}^{e_{10}}$ are presented in the appendix A.

2.2 Two-qubit mixed initial state

The state vector representation is only suitable for pure states. In this subsection we use the completely-positive trace-preserving (CPTP) map based on density matrices to describe the recovery control. To apply the proposed feed-forward recovery control in the case of the mixed initial state, we consider a completely-positive trace-preserving (CPTP) map, which acts on a two-qubit density matrix. Hence, the non-normalized final recovered state corresponding to measurement operator $M_{ij}(i,j = 0,1)$ is given as:

$$\begin{aligned}C(\bar{\rho}_{M_{ij}}^{fin}) &= \sum_{m,n=0}^{1} N_{ij}F_{ij}e_{mn}F_{ij}M_{ij}\rho_{in}\left(N_{ij}F_{ij}e_{mn}F_{ij}M_{ij}\right)^{\dagger} \\ &= \sum_{m,n=0}^{1} N_{ij}F_{ij}e_{mn}F_{ij}M_{ij}\rho_{in}M_{ij}^{\dagger}F_{ij}^{\dagger}e_{mn}^{\dagger}F_{ij}^{\dagger}N_{ij}^{\dagger}\end{aligned} \tag{18}$$

where N_{ij} are the post-weak measurement operators, F_{ij} are the feed-forward operations, M_{ij} are the pre-weak measurement operators given in Table. 1. Moreover, $e_{mn}, m,n = 0,1$ are four different Kraus operators for amplitude damping noise given

in Eq. (4). The probability for gaining the result $\bar{\rho}_{M_{ij}}$ is the normalization factor of Eq. (18) as:

$$\bar{g}_{M_{ij}}^{fin} = \sum_{m,n=0}^{1} trace\left(N_{ij}F_{ij}e_{mn}F_{ij}M_{ij}\rho_{in}M_{ij}^{\dagger}F_{ij}^{\dagger}e_{mn}^{\dagger}F_{ij}^{\dagger}N_{ij}^{\dagger}\right) \tag{19}$$

The total success probability for mixed initial states is given by substituting Eq. (19) in Eq. (10).

Since the initial and final states are both mixed, we find the fidelity corresponds to each measurement operator M_{ij} as:

$$\overline{Fid}_{M_{ij}} = \left[Tr\left(\sqrt{\sqrt{\bar{\rho}_{M_{ij}}^{fin}}\bar{\rho}_{in}\sqrt{\bar{\rho}_{M_{ij}}^{fin}}}\right)\right]^2 \tag{20}$$

The total fidelity for mixed initial state is defined by substituting Eq. (20) in Eq. (12).

2.3 Complete recovery condition of feed-forward control

As we explained in subsection A, the state of the system after passing through the amplitude damping noise channel will be in 'jump' or 'no jump' scenario. If one of the qubits or both of them jump, we are not able to retrieve the information of the initial state. However, when 'no jump' scenario takes place for both qubits by selecting the appropriate measurement strength for the post-weak measurements, one can make the state of the system after post-weak measurement $\left|\psi_{N_{ij}}^{e_{00}}\right\rangle$, completely same as the initial state $|\psi_{in}\rangle$. The state $\left|\psi_{N_{00}}^{e_{00}}\right\rangle$ given in Eq. (16) is the final state of the system for measurement operator M_{00} when no jump takes place for both qubits. It should be equal to the initial state of the system given in Eq. (1). Hence, all the vectors must be equal as: $p(1-q) = \sqrt{p}\sqrt{1-p}\sqrt{1-r}\sqrt{1-q} = \sqrt{p}\sqrt{1-p}\sqrt{1-r}\sqrt{1-q} = (1-p)(1-r)$, therefore, the complete recovery condition can be obtained as:

$$q = 1 - \frac{(1-p)(1-r)}{p} \tag{21}$$

which is a function of damping probability r and pre-weak measurement strength p.

We emphasize that in this paper we will frequently use Eq. (21) as the complete recovery condition. The complete recovery condition is the same for pure and mixed initial states. In fact, the complete recovery condition is independent of initial state.

Here we show that under complete recovery condition obtained in Eq. (21), the state $\left|\psi_{N_{00}}^{e_{00}}\right\rangle$ given in Eq. (16) will be exactly same as initial state.

By substituting the post-weak measurement strength q as Eq. (21), the state of the system given in Eq. (16) becomes:

$$\begin{aligned}\left|\widetilde{\psi}_{N_{00}}^{e_{00}}\right\rangle &= \frac{1}{\sqrt{\widetilde{g}_{N_{00}}^{e_{00}}}}\Big(\alpha(1-p)(1-r)|00\rangle \\ &+\beta(1-p)(1-r)|01\rangle \\ &+\gamma(1-p)(1-r)|10\rangle \\ &+\delta(1-p)(1-r)|11\rangle\Big) \\ &= \frac{(1-p)(1-r)}{\sqrt{\widetilde{g}_{N_{00}}^{e_{00}}}}\left(\alpha|00\rangle+\beta|01\rangle+\gamma|10\rangle+\delta|11\rangle\right)\end{aligned} \tag{22}$$

with probability

$$\begin{aligned}\widetilde{g}_{N_{00}}^{e_{00}} &= |\alpha|^2(1-p)^2(1-r)^2+|\beta|^2(1-p)^2(1-r)^2 \\ &+|\gamma|^2(1-p)^2(1-r)^2+|\delta|^2(1-p)^2(1-r)^2 \\ &= (1-p)^2(1-r)^2\left(|\alpha|^2+|\beta|^2+|\gamma|^2+|\delta|^2\right) \\ &= (1-p)^2(1-r)^2\end{aligned} \tag{23}$$

By substituting Eq. (23) in Eq. (22), the state $\left|\widetilde{\psi}_{N_{00}}^{e_{00}}\right\rangle$ becomes:

$$\begin{aligned}\left|\widetilde{\psi}_{N_{00}}^{e_{00}}\right\rangle &= \frac{(1-p)(1-r)}{\sqrt{(1-p)^2(1-r)^2}}\left(\alpha|00\rangle+\beta|01\rangle+\gamma|10\rangle+\delta|11\rangle\right) \\ &= \alpha|00\rangle+\beta|01\rangle+\gamma|10\rangle+\delta|11\rangle = |\psi_{in}\rangle\end{aligned} \tag{24}$$

Hence, one can see from Eq. (24) that the final state becomes exactly same as the initial state.

The same process occurs for the final states of all measurement operators $\left|\psi_{N_{ij}}^{e_{00}}\right\rangle$, when "no jump" scenario happens for both qubits. Therefore, under complete recovery condition obtained in Eq. (21), when "no jump" scenario happens for both qubits, one can completely recover the state of the system, for all measurement operators.

Under the complete recovery condition obtained in Eq. (21), we can obtain the complete recovery total success probability as follows. By substituting Eq. (21) in Eq. (11), the complete recovery total success probability becomes:

$$g_{total}(p,r) = \frac{(1-p)^2(1-r)^2(2p+r-pr)^2}{p^2} \tag{25}$$

According to Eq. (25), the total success probability under the complete recovery condition is not a function of the initial state; therefore, the behavior of the total success probability is the same for mixed and pure initial states.

3 Experiments and Discussions

In this section we study the performance of the proposed scheme in two cases: a) general recovery control, b) complete recovery control. In general recovery control the variables in recovery control such as pre-weak measurement strength p and post-weak measurement strength q have independent amounts. However, in complete recovery control, we use complete recovery condition in Eq. (21), where post-weak measurement strength q is a function of pre-weak measurement strength p and damping probability r.

For each recovery control scheme we study the behavior of total success probability and total fidelity.

3.1 General recovery control numerical experiments

In this subsection, we consider the general recovery control for two-qubit, in which the variables of pre-weak measurement strength p and post-weak measurement strength q have independent values.

The final expression for total success probability as a function of pre-weak measurement strength p, post-weak measurement strength q and damping probability r is given in Eq. (11). Fig. 2 depicted the total success probability given in Eq. (11), in general recovery scheme for a fixed amount of damping probability $r = 0.5$.

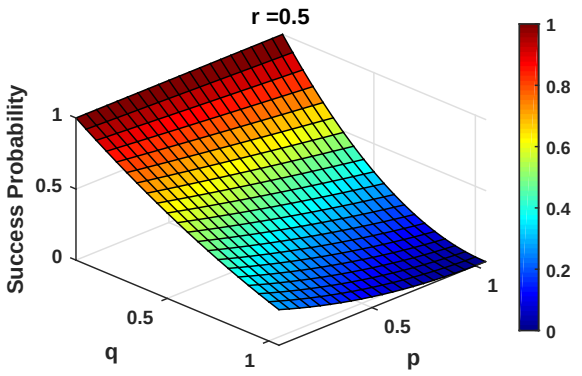

Fig. 2 General recovery total success probability as a function of pre-weak measurement strength p and post-weak measurement strength q for a fixed amount of damping probability $r = 0.5$.

As Fig. 2 shows, in general recovery control, post-weak measurement strength has the most significant effects on the behavior of success probability. By selecting weaker post-weak measurement strength, one can gain higher total success probability.

Since the analytical expression for the total fidelity as a function of (p,q,r) in general recovery control is complicated, we use the simulation experiments to study

the behavior of the fidelity. The total fidelity as a function of post-weak measurement and pre-weak measurement strength for a fixed amount of damping probability $r = 0.5$ via Monte-Carlo method for pure and mixed initial states are given in Fig. 3.

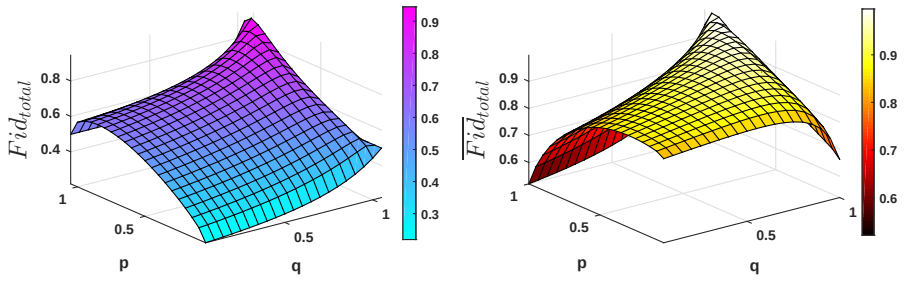

(a) Pure initial states.

(b) Mixed initial states.

Fig. 3 General recovery total fidelity as a function of pre-weak measurement and post-weak measurement strength for pure and mixed initial state for a fixed amount of damping probability $r = 0.5$ via Monte-Carlo method.

As Fig. 3 illustrates, to gain higher fidelity one needs to apply stronger post-weak measurement and pre-weak measurement for both pure and mixed initial states. However, the general recovery total fidelity for mixed initial states is higher than the total fidelity for pure initial states. The highest amount of total fidelity for pure initial states is $Fid_{total} = 91.32\%$, where its amount for mixed initial states is $\overline{Fid}_{total} = 99.63\%$

3.2 Complete recovery control numerical experiments

In this subsection we study the performance of the recovery control under complete recovery condition Eq. (21).

The complete recovery success probability is given in Eq. (25). To study the behavior of the complete recovery total success probability, we set the value of post-weak measurement strength q as complete recovery condition in Eq. (21), and use Monte-Carlo method over a large ensemble of two-qubit initial states. The complete recovery total success probability as a function of pre-weak measurement strength p and damping probability r for pure and mixed initial states via Monte-Carlo method is given in Fig. 4.

As can be seen from Fig. 4, in complete recovery control the success probability has the most significant value while the pre-weak measurement strength is so weak. By increasing the amount of pre-weak measurement strength the amount of total success probability decreases and tends to zero. We note that in complete recovery control, according to Eq. (21) q is the function of pre-weak measurement p and damping probability r. Since $q \geq 0$ the lowest amount of p depends on damping probability r. That's why in Fig. 4 there are some gaps in the amount of success probability for the small pre-weak measurement strength p.

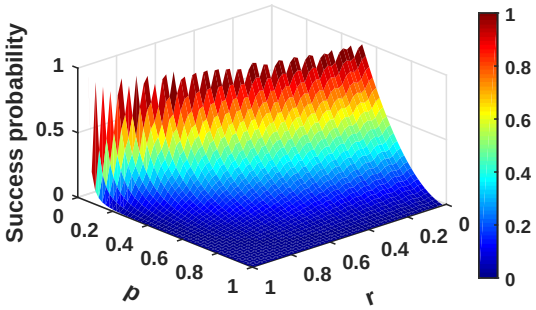

Fig. 4 Complete recovery total success probability as a function of pre-weak measurement strength and damping probability.

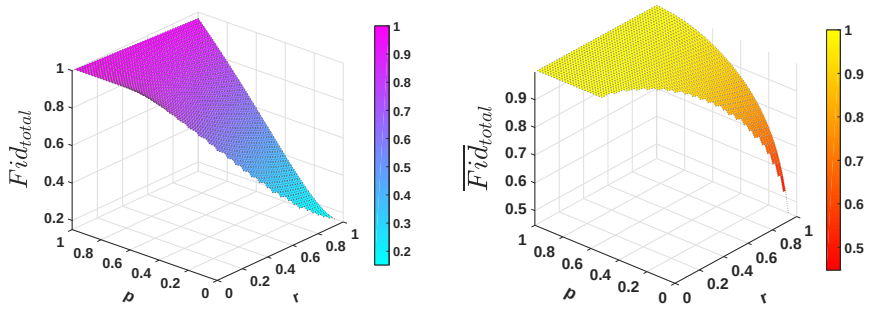

(a) Pure initial states. (b) Mixed initial states.

Fig. 5 Complete recovery total fidelity as a function of pre-weak measurement and damping probability for pure and mixed initial state via Monte-Carlo method.

The final expression for complete recovery total fidelity is too long, so the behavior of the fidelity is explained in numerical simulations. The behavior of the complete recovery total fidelity as a function of pre-weak measurement strength and damping probability for pure and mixed initial states via Monte-Carlo method are given in Fig. 5. We generate random initial pure and mixed states according to Haar measure of SU(4) by using MATLAB toolbox QETLAB [28], and change the amount of damping probability r and pre-weak measurement strength p uniformly from 0 to 1. Five steps of the recovery control described in Sec. II are applied on the random initial states. The total fidelity calculated according to Eq. (12). The averaged total fidelity over all random generated initial states are given in Fig. 5. Fig. 5(a) is the median value of the complete recovery total fidelity for pure initial states as in Eq. (12) and Fig. 5(b) is the median value of complete recovery total fidelity for mixed initial states by substituting Eq. (20) in Eq. (12).

Complete recovery total fidelity increases by adding the amount of pre-weak measurement strength as shown in Fig. 5. In a way that for $p \approx 1$ one can get the total fidelity close to 1 for both pure and mixed initial states. However, the fidelity of the complete recovery control is better in case of mixed initial states. It can be seen from

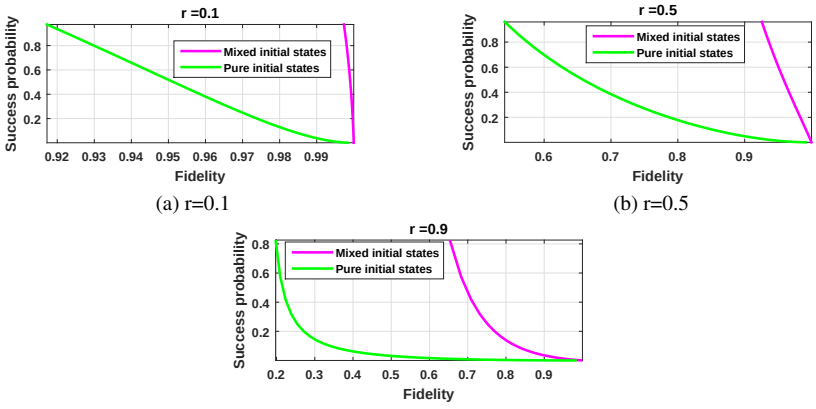

(a) r=0.1 (b) r=0.5

(c) r=0.9

Fig. 6 The relation between total fidelity and total success probability under complete recovery condition for (r=0. 01, 0.5 and 0.9) . Green curves correspond to pure initial states and magnet curves to mixed initial states.

Fig. 5(b) that the fidelity of mixed initial states is more than 99% for all amounts of damping probability by choosing the appropriate amount of pre-weak measurement. As one can see from Fig. 5 the behaviors of fidelity for mixed and pure initial states are different, so the total fidelity is dependent on initial state. However, the total success probability as given in Eq. (25) is independent of initial state.

Furthermore, to show the effectiveness of our recovery control for pure and mixed initial state, Fig. 6 illustrates the relation between total fidelity and total success probability via Monte Carlo method over 10^4 iterations of the two-qubit mixed and pure initial states. Once more, the complete recovery total fidelity for pure initial states is given in Eq. (12), and the complete recovery total fidelity for mixed initial states calculated by substituting Eq. (20) in Eq. (12). The complete recovery total success probability is given in Eq. (25). In each plot, the damping probability r is fixed as $r = 0.1$, 0.5 and 0.9, and the pre-weak measurement strength p changes from 0 to 1.

From Fig. 6, one can see that the higher the fidelity is, the lower success probability becomes, and vice versa. However, even for heavy damping probability our control scheme can protect two-qubit pure and mixed states from noise. By comparing the relation between total success probability and total fidelity of mixed and pure initial states, one can see the proposed feed-forward control has the same success probability but better fidelity for mixed initial states.

In order to compare the effectiveness of our recovery control for protecting two-qubit against amplitude damping, we demonstrate the total fidelity and total success probability in complete recovery condition and the control scheme in ref. [23]. In ref. [23], the Hadamard gate angle is a function of damping probability to get the best result of the control. In our paper, the complete recovery condition Eq. (21) is used to get the best result of the control, so the performance comparisons between these two control schemes are fair. Also, in ref. [23] the amplitude damping caused by weak measurement has been considered, which is equivalent to ‘no jump’ scenario for both qubits in our paper. Hence, we only consider the case of ‘no jump’ scenario.

For each amount of damping probability r, the best pre-weak measurement p is chosen for calculating the complete recovery total fidelity and complete recovery total success probability. As showed in Fig. 4 and Fig. 5 the highest fidelity is obtained with stronger pre-weak measurement and highest success probability is obtained with weaker pre-weak measurement. We generate arbitrary two-qubit pure states density matrices via extensive Monte-Carlo method over 10^4 iterations. Success probability as a function of damping probability for our complete recovery control Eq. (25) and recovery control in ref. [23] are shown in Fig. 7.

As demonstrated in Fig. 4, we need to choose the weakest possible pre-weak measurement strength p to gain the maximum success probability. According to complete recovery condition Eq. (21), the post-weak measurement strength q is a function of pre-weak measurement strength p and damping probability r. Since $q \geq 0$, the smallest amount of pre-weak measurement strength p depends on r and is different for each amount of damping probability r. That's why in Fig. 7 the amount of success probability is varied for different damping probabilities and even higher for intense damping probabilities.

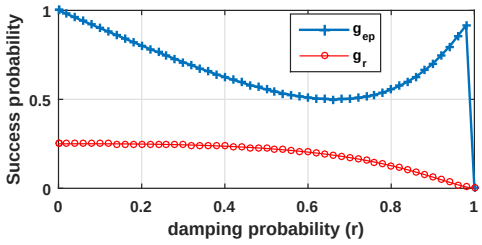

Fig. 7 Success probability as a function of damping probability r via Monte-Carlo method. The red curve is the success probability for protecting scheme in ref. [23]; and blue curve is the complete recovery total success probability of our scheme.

From Fig. 7 we can see that by choosing the appropriate amount of pre-weak measurement strength p, our control with complete recovery condition makes significant improvement for success probability even for the high amount of damping probability.

In addition, the fidelity as a function of damping probability via Monte-Carlo method is shown in Fig. 8. F_d is the fidelity between damped state and the initial state, without any control field; F_r corresponds to the fidelity of the recovery control in ref. [23]; and F_{ep} is the total fidelity of our control with complete recovery condition. Since we choose the strongest pre-weak measurement strength, fidelity of our control is close to 1 for all amounts of damping probability.

Also, to compare the amount of success probability (fidelity) for the given fidelity (success probability), we plot the relation between fidelity and success probability for our recovery control with the complete recovery condition and the recovery control in ref. [23] in Fig. 9. To make sure that our comparison is not just for some suitable states we use Monte-Carlo method over 10^4 iterations. The amount of damping probability varies from 0 to 1, and each point represents the corresponding amount of fidelity

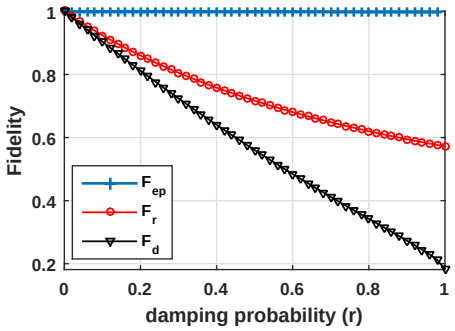

Fig. 8 Fidelity as a function of damping probability r via Monte-Carlo method. The black curve is the fidelity without any control field, the red curve is the fidelity for the control scheme in ref. [23]; and the blue curve is the total fidelity of our scheme with the complete recovery condition.

and success probability. The pre-weak measurement strength was chosen to be the smallest amount for each damping probability amount based on Eq. (21).

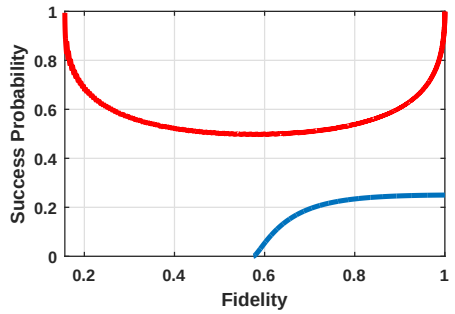

Fig. 9 The relation between fidelity and success probability via Monte-Carlo method. The red curve corresponds to our scheme and blue curve is for the control scheme in ref. [23].

As Fig. 9 depicted, our recovery control always has significant improvement in terms of success probability (fidelity) for the given fidelity (success probability).

3.3 Comparison between general recovery control and complete recovery control

We derive the complete recovery condition Eq. (21) to make the final state same as initial state in case that "no jump" scenario happens for one or both qubits. The question here arises as how effective is the complete recovery condition. To answer this question, in this subsection, we compare the performance of the complete recovery and general recovery control. As we show in subsections A and B, there is a trade-off between fidelity and success probability. Hence, the relation between fidelity and success probability is used to compare the general recovery control and complete recovery control.

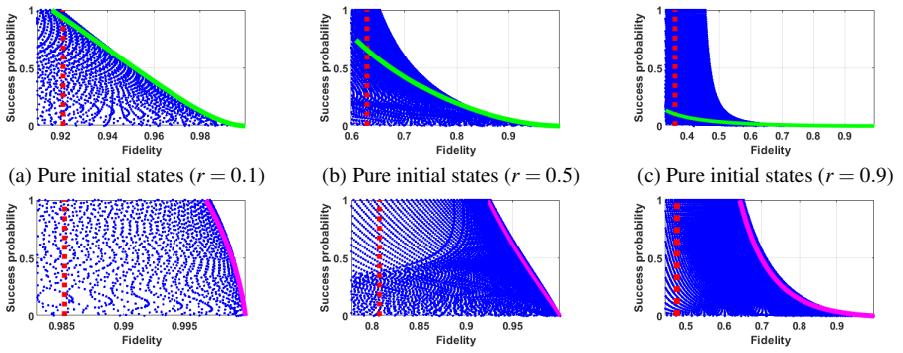

(a) Pure initial states ($r = 0.1$) (b) Pure initial states ($r = 0.5$) (c) Pure initial states ($r = 0.9$)

(d) Mixed initial states ($r = 0.1$) (e) Mixed initial states ($r = 0.5$) (f) Mixed initial states ($r = 0.9$)

Fig. 10 The relation between total fidelity (Fid_{total}) and total success probability (g_{total}) for pure and mixed initial states in general recovery control and complete recovery control via Monte-Carlo method. The green curve corresponds to complete recovery control for pure states and the magnet curve corresponds to complete recovery control for mixed states. The dashed red line represents the fidelity without any measurement and control.

Fig. 10 is the relation between total fidelity (Fid_{total}) and total success probability (g_{total}) via Monte-Carlo method. The amount of damping probability is fixed as $r = 0.5$. The blue dots demonstrate the performance of general recovery control for all independent real amounts of (p, q) from 0 to 1. The green curve corresponds to complete recovery control for pure states and the magnet curve corresponds to complete recovery control for mixed states which is given in Fig. 6 . The dashed red line represents the fidelity without any measurement and control.

For each amount of fidelity, the maximized success probability is located on the boundary of the diagram. Hence, the maximized fidelities and success probabilities are distributed on the boundary line of the diagram. Each point on the boundary line has a group of measurement strength (p, q) amount which one can gain the highest amount of success probability and corresponding fidelity.

As Fig. 10 depicted, for pure initial states, the performance of the complete recovery control (green curve) is close to highest amount of performance in general recovery control only for weak damping probabilities. However, the complete recovery control for mixed initial states (magnet curve) gains highest performance even for intense damping probabilities $r = 0.9$. Hence, for mixed initial states, the proposed complete recovery control gains the highest total success probability and total fidelity for all amounts of damping probability. While for pure initial states, the complete recovery control has the highest performance only for weak damping probabilities.

4 Conclusion

In this paper, we proposed a feed-forward control and its reversal to protect the arbitrary initial state of two-qubit system. The aim of the feed-forward operation is to make the state of the system robust to the amplitude damping. We consider the recovery in two cases: a) two-qubit pure initial state and b) two-qubit mixed initial state.

Fidelity and success probability were calculated to evaluate the performance of the control. Theoretical expressions were derived, and specific numerical results were illustrated in plots. We have shown that under complete recovery condition the state of the system can be completely recovered. The behavior of the performance of the proposed control scheme were studied for different initial state situations. Furthermore, we showed that the complete recovery control gains the maximum fidelity and success probability in case of mixed initial states, even for intense damping probabilities. We have demonstrated that: 1) The recovery scheme proposed in this paper is applicable for any arbitrary initial two-qubit state, which can gain complete fidelity even for heavy damping probabilities, by choosing the appropriate amounts for the variables in recovery control; 2) The complete recovery condition is independent of initial state; 3) The total success probability is independent of initial state; 4) The total fidelity is dependent on initial state. Our scheme has applications in quantum key distribution (QKD) protocols [29–31] where the state needs high tolerance to the noise of a communication channel.

A Appendix

Here we give the states of the system after the noise channel in case that the result $|00\rangle$ corresponding to M_{00} is acquired and after the noise channel just one of the qubits 'jump'.

If the first qubit 'no jump' and the second qubit 'jump', the state of the system becomes:

$$\left|\psi_{M_{00}}^{e_{01}}\right\rangle = \frac{1}{g_{e_{01}}}\left(\beta\sqrt{p}\sqrt{1-p}\sqrt{r}|00\rangle + \delta\sqrt{r}\sqrt{1-r}(1-p)|10\rangle\right) \tag{A1}$$

with probability $g_{e_{01}} = \beta^2 p(1-p)r + \delta^2 r(1-r)(1-p)^2$.

After the noise channel by applying the reversed operationF_{00}, the state of the system becomes: $\left|\psi_{F_{00}}^{e_{01}}\right\rangle = F_{00}|\psi^{e_{01}}\rangle = |\psi^{e_{01}}\rangle$.

At last, after the post-weak measurement the recovered state of the system represented as:

$$\left|\psi_{N_{00}}^{e_{01}}\right\rangle = \frac{1}{g_{e_{01}}^{N_{00}}}\left(\frac{\beta(1-p)\sqrt{1-p}\sqrt{r}(1-r)}{\sqrt{p}}|00\rangle + \frac{\delta\sqrt{r}(1-r)(1-p)\sqrt{1-p}}{\sqrt{p}}|10\rangle\right) \tag{A2}$$

with success probability:

$$g_{e_{01}}^{N_{00}} = \frac{\beta^2(1-p)^3 r(1-r)^2 + \delta^2 r(1-r)^2(1-p)^3}{p}.$$

In the case that first qubit 'jump' and second qubit 'no jump', the state of the system after the noise channel is: $\left|\psi_{M_{00}}^{e_{10}}\right\rangle = \frac{1}{g_{e_{10}}}\left(\gamma\sqrt{p}\sqrt{1-p}\sqrt{r}|00\rangle + \delta\sqrt{r}\sqrt{1-r}(1-p)|01\rangle\right)$ with probability $g_{e_{10}} = \gamma^2 p(1-p)r + \delta^2 r(1-r)(1-p)^2$.

After the feed-forward operation, the state of the system becomes $\left|\psi_{F_{00}}^{e_{10}}\right\rangle = F_{00}|\psi^{e_{10}}\rangle = |\psi^{e_{10}}\rangle$.

Finally, to recover the state of the system, we apply the post-weak measurement which makes the state of the system as:

$$\left|\psi_{N_{00}}^{e_{10}}\right\rangle = \frac{1}{g_{e_{10}}^{N_{00}}}\left(\frac{\gamma(1-p)\sqrt{1-p}\sqrt{r}(1-r)}{\sqrt{p}}|00\rangle + \frac{\delta\sqrt{r}(1-r)(1-p)\sqrt{1-p}}{\sqrt{p}}|01\rangle\right) \tag{A3}$$

with success probability:

$$g_{e_{10}}^{N_{00}} = \frac{\gamma^2(1-p)^3 r(1-r)^2 + \delta^2 r(1-r)^2(1-p)^3}{p}.$$

References

1. Cong, S.: Control of Quantum Systems: Theory and Methods. John Wiley & Sons (2014)
2. Chen, M., Kuang, S., Cong, S.: Rapid Lyapunov control for decoherence-free subspaces of Markovian open quantum systems. J. Franklin Inst. 354, 439–455 (2017)
3. Lu, F., Marinescu, D.C.: Quantum error correction of time-correlated errors. Quantum Inf. Process. 6, 273–293 (2007)
4. Grassl, M., Kong, L., Wei, Z., Yin, Z.-Q., Zeng, B.: Quantum error-correcting codes for qudit amplitude damping. IEEE Trans. Inf. Theory. 64, 4674–4685 (2018)
5. Wilde, M.M., Fattal, D.: Nonlocal quantum information in bipartite quantum error correction. Quantum Inf. Process. 9, 591–610 (2010)
6. Ofek, N., Petrenko, A., Heeres, R., Reinhold, P., Leghtas, Z., Vlastakis, B., Liu, Y., Frunzio, L., Girvin, S.M., Jiang, L.: Extending the lifetime of a quantum bit with error correction in superconducting circuits. Nature. 536, 441 (2016)
7. Cramer, J., Kalb, N., Rol, M.A., Hensen, B., Blok, M.S., Markham, M., Twitchen, D.J., Hanson, R., Taminiau, T.H.: Repeated quantum error correction on a continuously encoded qubit by real-time feedback. Nat. Commun. 7, (2016)
8. Mancini, S., Wang, J.: Towards feedback control of entanglement. Eur. Phys. J. D. 32, 257–260 (2005). doi:10.1140/epjd/e2004-00187-x
9. Rafiee, M., Nourmandipour, A., Mancini, S.: Optimal feedback control of two-qubit entanglement in dissipative environments. Phys. Rev. A. 94, 1–7 (2016). doi:10.1103/PhysRevA.94.012310
10. Rafiee, M., Nourmandipour, A., Mancini, S.: Universal feedback control of two-qubit entanglement. Phys. Rev. A. 96, 1–7 (2017). doi:10.1103/PhysRevA.96.012340
11. Yamamoto, N., Mikami, T.: Entanglement-assisted quantum feedback control. Quantum Inf. Process. 16, 179 (2017)
12. Wang, C., Xu, B., Zou, J., He, Z., Yan, Y., Li, J., Shao, B.: Feed-forward control for quantum state protection against decoherence. Phys. Rev. A. 89, 032303 (2014). doi:10.1103/PhysRevA.89.032303
13. Wakamura, H.: Noise suppression by quantum control before and after the noise. Phys. Rev. A - At. Mol. Opt. Phys. 022321, 1–9 (2017). doi:10.1103/PhysRevA.95.022321
14. Wakamura, H., Kawakubo, R., Koike, T.: State protection by quantum control before and after noise processes. Phys. Rev. A. 96, 1–7 (2017). doi:10.1103/PhysRevA.96.022325
15. Harraz, S., Yang, J., Li, K., Cong, S.: Quantum state transfer control based on the optimal measurement. Optim. Control Appl. Methods. 38(5): 744-753 (2017).
16. Brańczyk, A.M., Mendonça, P.E.M.F., Gilchrist, A., Doherty, A.C., Bartlett, S.D.: Quantum control of a single qubit. Phys. Rev. A. 1–11 (2007). doi:10.1103/PhysRevA.75.012329.
17. Gillett, G.G., Dalton, R.B., Lanyon, B.P., Almeida, M.P., Barbieri, M., Pryde, G.J., O'Brien, J.L., Resch, K.J., Bartlett, S.D., White, A.G.: Experimental feedback control of quantum systems using weak measurements. Phys. Rev. Lett. 104, 3–6 (2010). doi:10.1103/PhysRevLett.104.080503
18. Xiao, X., Feng, M.: Reexamination of the feedback control on quantum states via weak measurements. Phys. Rev. A. 83, 2–5 (2011). doi:10.1103/PhysRevA.83.054301
19. Yang, Y., Zhang, X.Y., Ma, J., Yi, X.X.: Extended techniques for feedback control of a single qubit. Phys. Rev. A - At. Mol. Opt. Phys. 87, 1–7 (2013). doi:10.1103/PhysRevA.87.012333
20. Harraz, S., Cong, S., Shuang, F.: Quantum noise protection via weak measurement for quantum mixed states. 2018 IEEE 7th Data Driven Control Learn. Syst. Conf. , Enshi, China, 302-307 (2018).
21. Guo, L.S., Xu, B.M., Zou, J., Wang, C.Q., Li, H., Li, J.G., Shao, B.: Discriminating two nonorthogonal states against a noise channel by feed-forward control. Phys. Rev. A - At. Mol. Opt. Phys. 91, 1–11 (2015). doi:10.1103/PhysRevA.91.022321
22. Cao, Y., Tian, G., Zhang, Z., Yang, Y., Wen, Q., Gao, F.: Composite control for protecting two nonorthogonal qubit states against decoherence. Phys. Rev. A. 032313, 1–9 (2017). doi:10.1103/PhysRevA.95.032313
23. Liao, Z., Al-Amri, M., Zubairy, M.S.: Protecting quantum entanglement from amplitude damping. Proc. SPIE. 8875, 887506-887506–9 (2013). doi:10.1117/12.2023241

24. Esfahani, S.S., Liao, Z., Zubairy, M.S.: Robust quantum state recovery from amplitude damping within a mixed states framework. J. Phys. B At. Mol. Opt. Phys. 49, 155501 (2016). doi:10.1088/0953-4075/49/15/155501
25. Harraz, S., Cong, S., Kuang S., Optimal Noise Suppression of Phase Damping Quantum Systems via Weak Measurement, J. Syst. Sci. Complex, 32(5): 1264-1279 (2019).
26. Nielsen, M.A., Chuang, I.L.: Quantum computation and quantum information. Cambridge university press (2010)
27. Korotkov, A.N., Keane, K.: Decoherence suppression by quantum measurement reversal. Phys. Rev. A. 81, 40103 (2010)
28. Johnston, N.: QETLAB: A MATLAB toolbox for quantum entanglement, version 0.9, (2016)
29. Wang, L., Zhou, Y.-Y., Zhou, X.-J., Chen, X., Zhang, Z.: Erratum: Correction to: New scheme for measurement-device-independent quantum key distribution. Quantum Inf. Process. 18, (2019)
30. Wang, G., Li, Z., Qiao, Y., Chen, Z., Peng, X., Guo, H.: Light source monitoring in quantum key distribution with single-photon detector at room temperature. IEEE J. Quantum Electron. 54, 1–10 (2018)
31. Brandt, H.E.: Topical Review: Optimum Probe Parameters for Entangling Probe in Quantum Key Distribution. Quantum Inf. Process. 2, 37–79 (2003)